

Effects of higher-order dispersion on pulse splitting in the normal dispersion regime

Ayhan Demircan · Monika Pietrzyk · Uwe Bandelow

Received: 31 July 2007 / Accepted: 20 May 2008 / Published online: 10 June 2008
© Springer Science+Business Media, LLC. 2008

Abstract By solving numerically the extended nonlinear Schrödinger equation we investigate the influence of higher-order dispersion effects on the propagation of optical pulses in the normal dispersion regime in a highly nonlinear fiber. Already a small amount of third-order dispersion can lead to a pulse-breakup above a certain pulse power. The splitting is followed by an expansion of the spectrum towards longer wavelengths without any impact of Raman scattering. The transfer of energy to longer wavelengths strongly depends on the dispersion profile of the fiber.

Keywords Nonlinear fibers · Pulse splitting · Third-order dispersion

1 Introduction

The propagation of a pulse through a nonlinear, dispersive optical medium can result in considerable changes to its temporal and spectral properties, due to the interplay of different physical effects acting on the pulse. For example the supercontinuum generation in nonlinear fibers has been a subject of numerous investigations for years, see e.g. the review [Dudley et al. \(2006\)](#), both because of many applications of supercontinuum sources, as well as of the interesting nonlinear physics that is involved in the spectral broadening process. There is a variety of effects modifying the shape of a pulse and its spectrum, like soliton fission (SF), associated with the generation of dispersive waves ([Husakou and Herrmann 2001](#)), Raman scattering, modulation instability (MI) ([Demircan and Bandelow 2007](#)), and other four-wave-mixing processes. This situation makes it particularly difficult to identify the impact of each physical process in a specific physical experiment. However, in the anomalous dispersion regime SF and MI, which are described solely by the fundamental nonlinear Schrödinger equation (NLSE), turn out to be the basic mechanisms. This reflects how inherent properties

A. Demircan (✉) · M. Pietrzyk · U. Bandelow

Weierstraß-Institut für Angewandte Analysis und Stochastik (WIAS), Mohrenstrasse 39, 10117 Berlin
e-mail: demircan@wias-berlin.de
URL: <http://www.wias-berlin.de>

of the NLSE are of primary importance for the propagation dynamics, even for ultrashort pulse propagation in photonic-crystal fibers (PCF) with extremely high nonlinearity.

To avoid the influence of MI and soliton effects such as SF and self-frequency shift, the pump pulse can be injected within the normal dispersion regime, far from the zero-dispersion wavelength (ZDW). This enables one to investigate the effects of Raman-scattering. In addition, the normal dispersion regime provides parameter regions where the efficiency of four-wave mixing is reduced and the signature of a discrete Raman cascade can be clearly identified. Also the role of cross-phase modulation and parametric four-wave-mixing can be investigated (Agrawal 1995; Coen et al. 2002). But inherent propagation properties described by the fundamental NLSE are suppressed or superimposed by higher-order effects, so that it becomes difficult to isolate the relative contributions of the involved physical parameters.

We demonstrate how strongly even small dispersive effects can affect the propagation dynamics in a HNLF. A significant impact of third-order dispersion (TOD) is that the dispersion profile is covering normal and anomalous dispersion regimes. Then, already a small TOD can lead to a pulse-breakup above a critical pulse power. The splitting is followed by an expansion of the spectrum towards longer wavelengths with the evolution of a broad Stokes component and without any impact of Raman scattering. The Stokes frequency depends strongly on the third-order dispersion coefficient, which enables the transfer of energy to a broad range of longer wavelengths.

2 The role of higher-order dispersion

To investigate the effect of dispersion on the propagation dynamics, we have solved numerically the one-dimensional nonlinear Schrödinger equation with in addition $\text{TOD} \sim \beta_3$ and fourth-order dispersion (FOD) $\sim \beta_4$, for the slowly varying complex envelope $A(z, \tau)$ of a pulse which propagates along the z -axis within a retarded time frame $\tau = t - z/v_g$ with the group velocity v_g

$$\frac{\partial A}{\partial z} = -\frac{i}{2} \beta_2 \frac{\partial^2 A}{\partial \tau^2} + \frac{1}{6} \beta_3 \frac{\partial^3 A}{\partial \tau^3} + \frac{i}{24} \beta_4 \frac{\partial^4 A}{\partial \tau^4} + i\gamma |A|^2 A. \quad (1)$$

We exclude in our numerical investigations any contribution from phase-matched parametric four-wave mixing and from higher-order nonlinearities as Raman scattering or self-steepening. This corresponds to the situation of a highly nonlinear fiber (HNLF), with small input powers and pulse durations exceeding several picoseconds so that the spectral bandwidth is much smaller than the Raman frequency shift in fused silica, hence the pump pulses do not suffer significantly from intrapulse Raman scattering as in the femtosecond case. Our technique for solving Eq. 1 is based on a standard de-aliased pseudospectral method in which the dispersion parts are calculated in the frequency domain and the nonlinearity is calculated as a product in the time domain. The integration is performed for the whole equation in the frequency domain with an eighth-order Runge-Kutta integration scheme with adaptive stepsize control (Demircan and Bandelow (2005)). Figure 1 represents the simulated pulse shapes and spectra for an injected pulse $A(0, \tau) = \sqrt{P_0} \operatorname{sech}(\tau/\tau_0)$ in the normal dispersion regime at $z = 445\text{m}$ and $z = 545\text{m}$. The pulse shapes show that pulse splitting at the leading edge sets in at $z = 445\text{m}$. This pulse-breakup phenomenon in the normal dispersion regime is described in Demircan et al. (2006); Demircan and Bandelow (2006). The TOD leads to an asymmetric temporal development with an enhanced transfer of power from the trailing portion of the pulse to the leading one. A narrow peak builds up and an increase of the peak intensity at the front of the pulse can be observed. The spectrum develops with a small

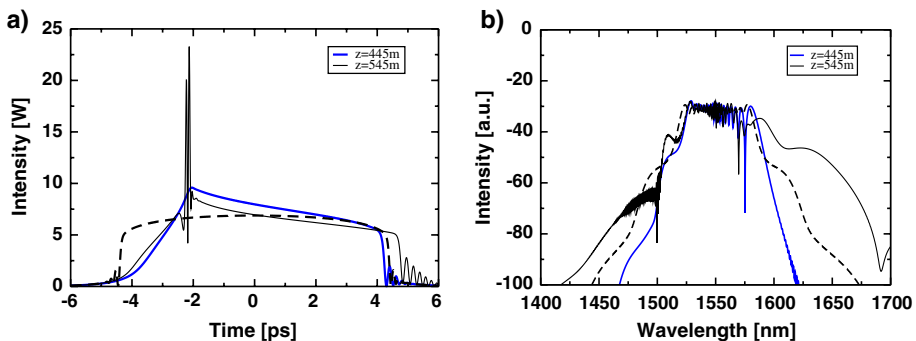


Fig. 1 Pulse shapes (a) and spectra (b) for injected sech^2 -pulses with $\tau_0 = 1.8\text{ ps}$ and $P_0 = 16\text{ W}$ in a fiber with $\beta_2 = 0.2\text{ ps}^2/\text{km}$, $\beta_3 = 0.01\text{ ps}^3/\text{km}$ and $\gamma = 10.5\text{ W}^{-1}\text{ km}^{-1}$ after $z = 445\text{ m}$ (blue) and $z = 545\text{ m}$ (black). The dashed black lines represent the simulation for the NLSE without TOD

asymmetric broadening towards the blue side. Further propagation as well as a higher peak power leads to a sharp increase of the peak intensity at the front of the pulse, which is halted by temporal pulse splitting. After the splitting a small pedestal on the red side of the spectrum appears.

The most important contribution of the TOD in the normal dispersion regime comes from the fact, that the dispersion profile $\beta(\omega)$ merges to the anomalous dispersion regime. Thereby soliton effects add, once the spectrum of the pulse touches the anomalous dispersion regime.

Figure 2 contrasts the propagation in the pure normal dispersion regime $\beta_2 = 0.2\text{ ps}^2/\text{km}$ (Fig. 2a, b) with the propagation in addition with $\beta_3 = 0.01\text{ ps}^3/\text{km}$ (Fig. 2c, d) and a reduced overlap with the anomalous dispersion regime in addition with $\beta_3 = 0.01\text{ ps}^3/\text{km}$ and $\beta_4 = 2 \times 10^{-4}\text{ ps}^4/\text{km}$, c.f. Fig. 3a. In Fig. 2a, b the pulse evolves first into a parabolic shape and broadens with further propagation nearly to a rectangular shape, thereby exhibiting optical wave breaking. In this case the spectrum is mainly broadened by self-phase modulation. Introducing TOD (Fig. 2c, d) for the same input pulse leads to the pulse splitting phenomenon. The spectrum is asymmetrically pronounced on the blue side, but also exhibits a broad pedestal on the red side. After the splitting of the pulse the spectrum touches the anomalous dispersion regime (c.f. black curve in Fig. 3a) and the small pedestal on the red side of the spectrum increases with further propagation. This means that more energy is transferred into the anomalous dispersion region, such that soliton effects come into play, in addition to the generation of a Stokes component. The further propagation is now mainly influenced by soliton fission and by the generation of resonant dispersive waves, leading to a blue shift in the spectrum (Husakou and Herrmann 2001; Demircan and Bandelow 2007). To reduce the soliton effects and to suppress the spectral extension on the blue side we narrow the bandwidth of the anomalous dispersion region by switching on a small value of $\beta_4 (= 2 \times 10^{-4}\text{ ps}^4/\text{km})$ (c.f. blue curve in Fig. 3a). The overall observed behavior (Fig. 2e, f) corresponds to the case of $\beta_4 = 0$ described above, up to the point, where the pulse splitting phenomenon occurs. However, the pulse does not split into fundamental solitons like in Fig. 2c. Also its spectrum extends to the blue side less than in Fig. 2d, and is now more pronounced to the red side. The spectral width saturates after a certain propagation distance and remains in a well bounded domain with a fixed Stokes wavelength, which is located in the anomalous dispersion region. The final spectrum of the pulse is asymmetric with a pronounced red tail and the spectral shape exhibits a depleted region around the ZDW.

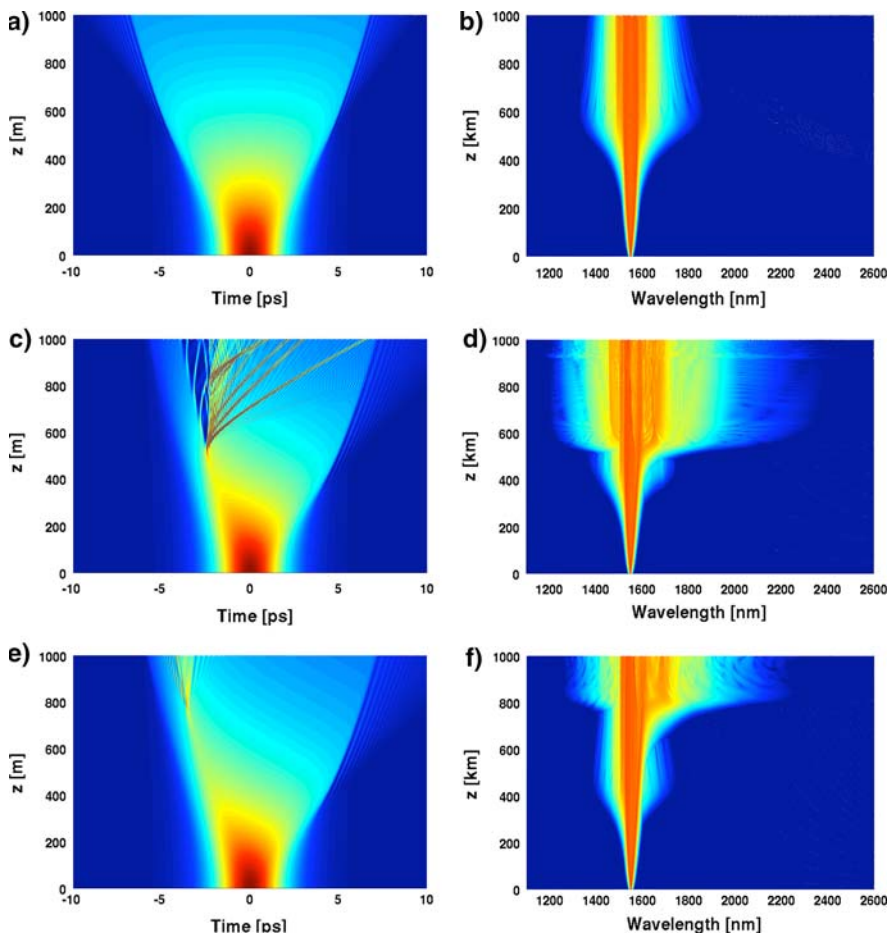


Fig. 2 Temporal (left) and spectral (right) evolution of a pulse with $\tau_0 = 1.8 \text{ ps}$ and $P_0 = 16 \text{ W}$ along 1 km HNLF with $\beta_2 = 0.2 \text{ ps}^2/\text{km}$ (a,b) $\beta_3 = 0$, $\beta_4 = 0$, (c,d) $\beta_3 = 0.01 \text{ ps}^3/\text{km}$, $\beta_4 = 0$ and (e,f) $\beta_3 = 0.01 \text{ ps}^3/\text{km}$, $\beta_4 = 2 \times 10^{-4} \text{ ps}^4/\text{km}$

Solitons can form only at frequencies within the anomalous dispersion regime, the bandwidth of which we can reduce by increasing β_4 . Figure 3 represents the behavior by a narrowing of the anomalous regime. Figure 3a shows the dispersion profiles for $\beta_4 = 2 \times 10^{-4} \text{ ps}^4/\text{km}$ and $\beta_4 = 3 \times 10^{-4}$ in comparison to the case without β_4 . Increasing P_0 leads to a pulse splitting after shorter propagation distances, because the pulse spectrum overlaps earlier with the anomalous dispersion regime, but broadens less to the red side.

Contrary to Raman scattering, where the Stokes component in fused silica is separated by $\approx 13 \text{ THz}$ from the pump frequency, the Stokes component here can be adjusted to an arbitrary wavelength on the red side with an appropriate dispersion profile design.

3 Conclusion

By numerically solving the extended nonlinear Schrödinger equation we have investigated the impact of higher-order dispersion on the propagation of optical pulses along highly non-

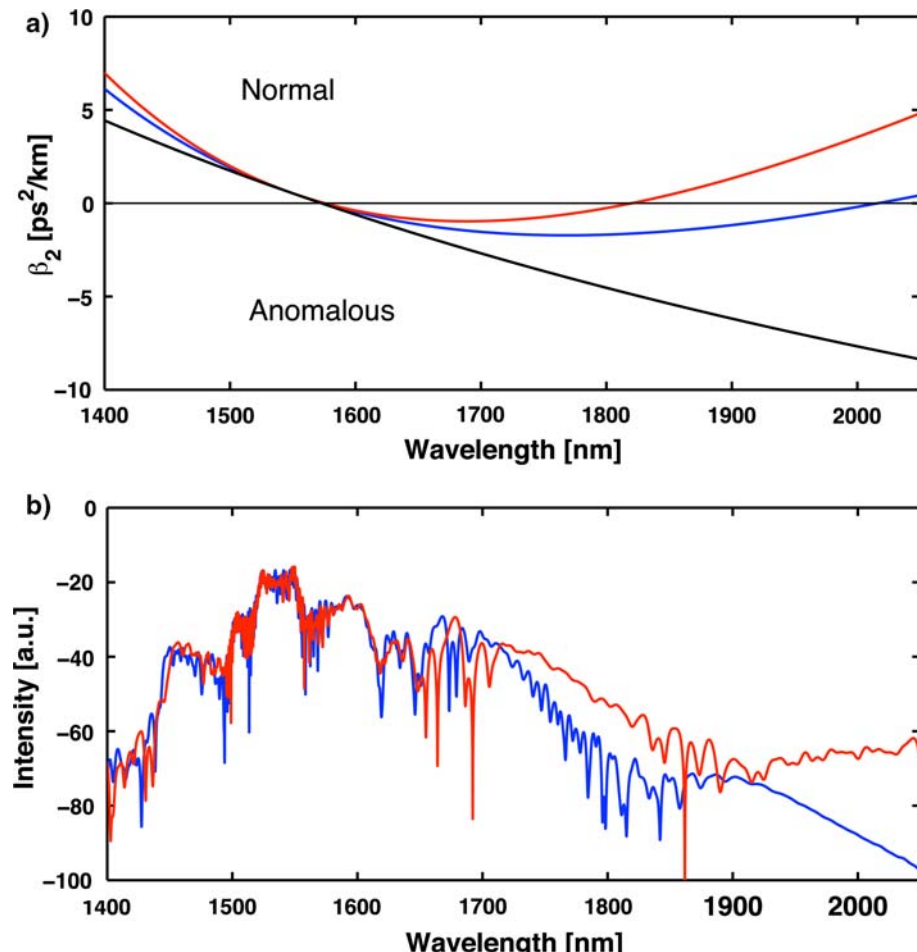


Fig. 3 (a) Dispersion profiles for $\beta_2 = 0.2 \text{ ps}^2/\text{km}$, $\beta_3 = 0.01 \text{ ps}^3/\text{km}$, without β_4 (black line) and with small values of β_4 : $\beta_4 = 2 \times 10^{-4} \text{ ps}^4/\text{km}$ (blue line), $\beta_4 = 3 \times 10^{-4} \text{ ps}^4/\text{km}$ (red line). (b) Spectra at $z = 158 \text{ m}$ and $P_0 = 64 \text{ W}$ for dispersion with $\beta_4 = 2 \times 10^{-4}$ (blue line) and $\beta_4 = 3 \times 10^{-4}$ (red line)

linear fibers. In the normal dispersion regime the initial spectral broadening of a pulse is dominated by self-phase modulation, whereas its further evolution depends sensitively on the underlying dispersion profile, either allowing for solitonic effects or not. In presence of TOD pulse splitting has been demonstrated, as well as its suppression later by fourth-order dispersion.

Acknowledgment The authors acknowledge the support by the projects D14 and D20 in the DFG Research Center MATHEON mathematics for key technologies.

References

Agrawal, G.P.: *Nonlinear Fiber Optics*. Academic, San Diego, CA (1995)
 Coen, S., Chau, A.H.L., Leonhardt, R., Harvey, J.D., Knight, J.C., Wadsworth, W.J., Russel, P.S.J.: Supercontinuum generation by stimulated Raman scattering and parametric four-wave mixing in photonic crystal fibers. *J. Opt. Soc. Am. B.* **19**, 753–764 (2002)

Demircan, A., Bandelow, U.: Supercontinuum generation by the modulation instability. *Opt. Commun.* **244**, 181–185 (2005)

Demircan, A., Bandelow, U.: Limit for pulse compression by pulse splitting. *Opt. Quant. Elect.* **38**, 1167–1172 (2006)

Demircan, A., Bandelow, U.: Analysis of the interplay between soliton fission and modulation instability in supercontinuum generation. *Appl. Phys. B* **86**, 31–39 (2007)

Demircan, A., Kroh, M., Bandelow, U., Hüttl, B., Weber, H.G.: Compresion limit by third-order dispersion in the normal dispersion regime. *IEEE Phot. Technol. Lett.* **18**, 2353–2355 (2006)

Dudley, J.M., Genty, G., Coen, S.: Supercontinuum generation in photonic crystal fiber. *Rev. Mod. Phys.* **78**, 1135–1184 (2006)

Husakou, A.V., Herrmann, J.: Supercontinuum generation of higher-order-solitons by fission in photonic crystal fibers. *Phys. Rev. Lett.* **87**, 203901 (2001)